Confocal Raman Microscopy of Optical-Trapped Particles in Liquids

Daniel P. Cherney and Joel M. Harris

Department of Chemistry, University of Utah, Salt Lake City, Utah 84112;
email: harrisj@chem.utah.edu

Annu. Rev. Anal. Chem. 2010. 3:277–97

First published online as a Review in Advance on March 9, 2010

The *Annual Review of Analytical Chemistry* is online at anchem.annualreviews.org

This article's doi:
10.1146/annurev-anchem-070109-103404

1936-1327/10/0719-0277$20.00

Key Words

Raman spectroscopy, colloid analysis, optical tweezers, microchemistry, emulsions, dispersions

Abstract

The in situ analysis of small, dispersed particles in liquids is a challenging problem, the successful solution to which influences diverse applications of colloidal particles in materials science, synthetic chemistry, and molecular biology. Optical trapping of small particles with a tightly focused laser beam can be combined with confocal Raman microscopy to provide molecular structure information about individual, femtogram-sized particles in liquid samples. In this review, we consider the basic principles of combining optical trapping and confocal Raman spectroscopy, then survey the applications that have been developed through the combination of these techniques and their use in the analysis of particles dispersed in liquids.

1. INTRODUCTION

1.1. Raman Spectroscopy for Analysis of Dispersed Particles

A variety of chemical materials are processed and delivered as dispersions of small particles in liquids. This technology finds widespread use in diverse areas, including aqueous suspensions of organic compounds, oligomers, and polymers for production of coatings, as well as inks, adhesives, and synthetic products, which do not require volatile organic solvents (1). Polymer colloids are employed for drug delivery (2) and as supports for combinatorial synthesis (3); dispersed inorganic solids are used in modifying the rheology of liquids (4) and in transport of insoluble molecules (5). Dispersed sols can be aggregated into porous structures that are useful as separation media, catalysts, or hosts for entrapped molecules for chemical sensing and other applications (6). Dispersions of colloidal structures are ubiquitous in molecular biology in the form of cells, bacteria, virus particles, or vesicles.

Despite the utility and widespread occurrence of colloidal dispersions, probing their structure, chemistry, and function represents a significant challenge for chemical analysis. Separation methods (7) and light scattering (8, 9) may be used to characterize particles by their size and surface-charge density. The shapes and sizes of particles can be determined ex situ by electron microscopy. Given the chemical complexity of colloidal materials, however, it is evident that size, shape, and surface charge do not provide sufficient information for us to understand these materials. Spectroscopic methods are needed to identify the composition and structure of colloidal particles and to probe their chemistry and reactivity. Unlike well-mixed liquid solutions, dispersed particles generally do not exchange material upon collision, so their compositions may be inhomogeneous and remain so over time. This particle-to-particle inhomogeneity implies that samples must be characterized at the individual-particle level. Finally, studies of the reactivity of colloids require an in situ method of analysis that allows observation of reactions of suspended particles in contact with solution.

Raman scattering spectroscopy (10, 11) provides a nearly ideal tool for investigating the chemical structure of colloidal particle dispersions. Because Raman scattering from water is weak, the technique is compatible with aqueous solutions typically used for particle dispersions. Excitation and scattering are typically in the visible or near-infrared region, which makes the technique compatible with optical fibers and microscopes, simplifying the development of instrumentation. A major drawback of Raman spectroscopy, however, is that the scattering cross sections are small—$\sigma \sim 2 \times 10^{-28}$ cm^2, or more than ten orders smaller than fluorescence-emission cross sections—which limits the technique's applicability to high-concentration samples. Conventional Raman scattering measurements of bulk particle suspensions are challenging, as illustrated in **Figure 1*a***, where the signals can be dominated by interferences from the solution unless very high particle densities are used. Even with high particle concentrations, no local information about the composition of particles relative to their surroundings can be obtained. These problems can be overcome by carrying out the Raman scattering measurement in an epi-illumination, confocal microscope, as shown in **Figure 1*b***, where a small detection volume is defined by the focused excitation laser beam and by imaging the collected scattering through a matched aperture (12). This detection volume is generally diffraction limited and small (~1 fl) and can be filled with a single particle in dilute dispersions. The resulting measurement provides local composition information about the particle, changes in which may be related to chemical reactions or exchange of bound molecules with the surrounding solution. The final challenge for observing individual particles in suspension is maintaining the particle within the small confocal detection volume. Brownian motion of small particles in low viscosity solvents is rapid, such that a 0.5-μm particle in water can diffuse out of a confocal detection volume in ~1 s.

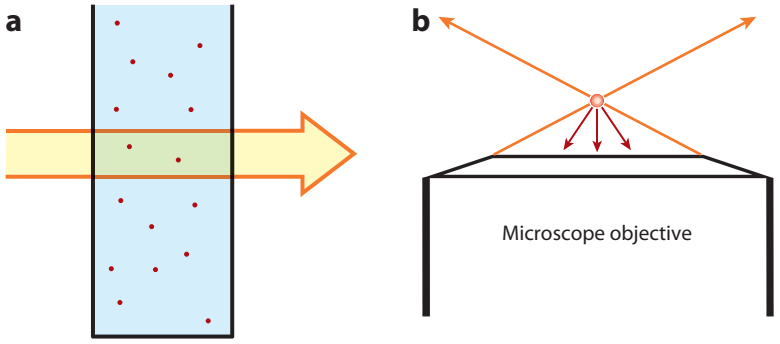

Figure 1

Raman spectroscopy of dispersed particle samples. (*a*) Conventional Raman spectroscopy of a dilute particle suspension. High-concentration dispersions are needed; otherwise, the observed scattering is dominated by the solution between the particles. (*b*) Confocal Raman microscopy of an individual particle. The detection volume is dominated by the particle, independent of the concentration of the dispersion. Raman scattering is collected by the same objective used to focus the laser beam in the sample.

1.2. Optical-Trapping Raman Microscopy

The problem of confining small particles within a small detection volume in confocal microscopy is readily solved by optical trapping, where interaction between tightly focused laser radiation and particles that have a refractive index greater than their surroundings leads to confinement of the particle to the laser focus (13–16). Optical traps, often referred to as laser tweezers, utilize a tightly focused laser that produces a large gradient in the electromagnetic (EM) field. Trapping occurs when the force and energy gradients on the particle that are present near the center of focus overcome gravitational forces and thermal energy to hold a sample near the focus of the optical trap. Since its discovery in 1970 (13), applications of optical trapping for manipulation of inorganic, organic, and biological particles have blossomed (17–23).

The first experiments combining optical trapping with Raman scattering measurements were applied to levitation and trapping of aerosol particles, both solid (glass, quartz) (24) and liquid droplets (25, 26), in the gas phase. These aerosols are generally several micrometers in diameter and have been studied to characterize their contents (26, 27), to observe evaporation characteristics (28), to monitor photopolymerization reactions (29, 30), and to obtain temperature measurements of trapped droplets over time (31, 32). Morphology-dependent optical resonances have been observed to occur in trapped liquid aerosol droplets due their well-defined, spherical shape (33). This shape leads to formation of standing waves that can modulate the intensity of peaks in the Raman spectrum and can provide size information about the particle (34). For an overview of optical levitation and trapping of aerosol particles combined with Raman spectroscopy, see References 34 and 35 and literature cited therein; aerosols in the gas phase are not covered in this review.

The focus of this article is the application of optical-trapping confocal Raman microscopy to particulate samples in liquids. The acquisition of a Raman spectrum of an optically trapped particle provides information through frequencies of vibration and their scattering intensities that can reveal molecular structure for femtogram amounts of material. The combination of optical trapping and Raman spectroscopy has proven to be powerful for the study of small, dilute dispersed particles whose Raman spectra are otherwise difficult to obtain due to their low concentrations in the sample. We present the basic principles of combining optical trapping and confocal Raman

spectroscopy, then survey the applications that have been developed through the combination of these techniques to analyze particles dispersed in liquid solutions.

2. EXPERIMENTAL METHODS

2.1. Optical Trapping of Particles in Liquids

The forces and energies involved in optical trapping are classified according to the size of the particle compared to the wavelength of light. For transparent particles whose size is greater than the wavelength of the trapping radiation light ($d_{\text{particle}} \gg \lambda_{\text{trapping}}$), a ray-optics picture can be used to understand the forces of trapping brought about by changes in momentum of scattered and refracted radiation. For smaller particles in the Rayleigh regime ($d_{\text{particle}} \ll \lambda_{\text{trapping}}$), which have a refractive index greater than the surrounding medium, the larger polarizability of the particle produces greater induced dipoles than the solvent and attracts the particle into the focused beam. Several thorough discussions of the theory of trapping for both regimes are available (14–16, 36–38). In this section, we briefly review the principles of single-beam optical traps and discuss examples as a point of reference for force and energy gradients involved in trapping of typical samples.

Optical trapping of particles larger than the wavelength of the trapping radiation is based on transfer of momentum from the incident radiation to the particle and may be described via a ray-optics model (13, 14). Although photons have no rest mass, they do carry momentum equal to $h\upsilon/c$ (where h is Planck's constant, υ is the photon's frequency, and c is the speed of light), and reflection or scattering of radiation by a particle transfers momentum to the particle. Reflection of a $P = 10$ mW beam can transfer a force of $2P/c \sim 70$ pN, which is 20 times greater than required to overcome the force of gravity on a 10-μm-diameter polystyrene sphere in water. Thus, only a fraction of the force available from momentum transfer of a modest-power laser beam is needed to levitate and trap large colloidal particles. **Figure 2** illustrates a spherical particle, whose refractive index is greater than its surroundings, trapped just above the focus of a laser beam. Radiation reflected or scattered downward transfers upward momentum to the particle, in the original

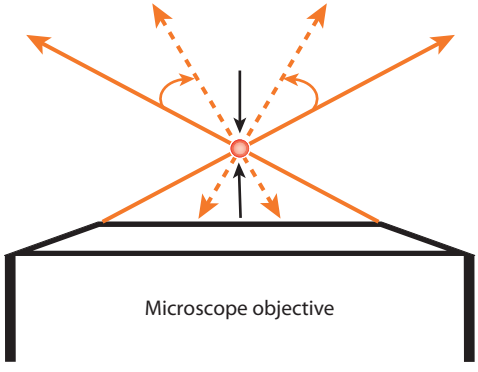

Figure 2

A ray-optics picture of the optical trapping of a spherical particle above the focus of a laser beam. Scattering and reflection of the laser beam back toward the source transfer momentum to the particle in the upward direction. Refraction of the diverging beam by the particle increases the light's momentum in the upward direction, transferring momentum downward on the particle. The forces depend on the position of the particle relative to the focus; these forces balance (*black arrows*) and lead to stable trapping.

direction of light propagation. If this were the only force, the particle would be ejected from the trap. However, due to the higher refractive index of the particle, the diverging laser beam is focused by the particle, which increases the light's momentum in the upward direction and transfers a downward force on the particle. There is a similar refraction effect when the particle is displaced laterally from the center of the focus (14), which directs light toward the direction of the displacement and transfers momentum to the particle to return it to the focus. The gradient forces in both the axial and the transverse directions are sensitive to the location of the particle relative to the laser focus, so the particle settles into a position at which the forces of gravity, scattering, and refraction are balanced.

The ray-optics model gives an intuitive picture of optical trapping of larger particles and is capable of providing quantitative predictions of trapping efficiencies for larger (>10-μm) particles (15) with accuracy degraded by approximately twofold for particles as small as the wavelength of the trapping radiation (36). However, for smaller particles trapped with tightly focused laser beams derived from high-numerical-aperture (NA) objectives, the assumptions of the ray-optics model break down, and an EM model (39) of the internal and external EM fields provides a much more accurate prediction of momentum transfer and the resulting trapping efficiencies (36).

For particles much smaller than the wavelength of the trapping radiation ($d_{\text{particle}} \ll \lambda_{\text{trapping}}$) in the Rayleigh scattering regime, the forces of optical trapping become a balance of (*a*) scattering by the particle, $F_{\text{scatter}} = (nP_{\text{scatter}})/c$, where the scattered power is predicted by the incident laser power and the Rayleigh scattering cross section, and (*b*) a gradient or dipole force, $F_{\text{grad}} = -\frac{1}{2}n\alpha \cdot \nabla E^2$, which depends on the volume polarizability of the particle, α; the refractive index of the medium, n; and the gradient in the radiation energy density, ∇E^2, which increases with tight focusing of the laser beam (14, 16). For smaller particles in tightly focused laser beams, the r^3 dependency of the volume polarizability causes the gradient force to dominate the Rayleigh scattering force, which decreases with a sixth-power dependency on r. The limit of trapping is then determined by whether the trapping energy is sufficient to overcome the thermal energy that gives rise to the Brownian motion of an unconstrained particle. Transferring a particle that is more polarizable than its surrounding solution into the center of the focused laser beam lowers the free energy of the system (14) by

$$\Delta G(z) = -\frac{1}{2}n\langle E^2(z)\rangle \delta\varepsilon v,$$

where $\langle E^2(z)\rangle$ is the energy density at the center of the laser focus, $\delta\varepsilon$ is the dielectric contrast between the particle and solution, and v is the particle volume. For a 10-mW laser beam focused to a radius ($w = 0.3$ μm), the predicted trapping energy of a 100-nm polystyrene particle in water at the center of the focused spot is $\Delta G(z) \approx -1.0 \times 10^{-19}$ J or ~25 kT. This result was verified by the successful trapping of 0.11-μm polystyrene latex particles with a ~12-mW laser beam (14) and illustrates that there is indeed sufficient energy available from modest-power lasers to trap submicrometer-sized particles and overcome their thermal motion.

2.2. Effects of Laser Radiation on Trapped Particles

Modest–laser power needs are advantageous, especially for trapping samples that have light-absorbing chromophores that can photobleach or heat the sample; in the case of living cells, the effects of heating can lead to cell death. Early experiments on optical trapping of bacteria showed that focused laser powers in excess of 100 mW at 514.5 nm were lethal to bacteria, although they could survive 5-mW trapping for periods of 10 min (17). Shorter-wavelength lasers can be damaging due to one- or two-photon excitation of electronic transitions in the tightly

focused beam, as illustrated by the effects of 488-nm radiation on trapped polystyrene particles (40, 41). To prevent photodamage by electronic excitation, investigators commonly use deep red and near-infrared lasers for trapping. Although these sources generally prevent direct photodamage, they can still heat the sample by excitation of vibrational overtones of water. Near a peak in the water overtone spectrum at 985 nm, a temperature rise of 4 K was measured at the center of a tightly focused 55-mW beam; this observation is in good agreement with the absorptivity of water (42). With a Nd:YAG laser operating at 1.06 μm, heating of the trap was measured by the thermal motion of trapped beads and was found to be only ~9.1 K W^{-1} (0.9 K per 100 mW power), due to the lower absorptivity of water (43) at this wavelength.

Single-beam optical traps can be used for Raman scattering measurements, where a tightly focused deep red (44) or near-infrared (45) laser beam both traps the particle and excites Raman scattering. Regarding samples that do not absorb at these longer wavelengths but that are soft and deformable, it is still advantageous to trap them with low laser powers to avoid particle deformation within the optical trap. Dynamic instabilities and changes in the membrane structure can be caused by optical trapping of lipid vesicles (46, 47); bending of a lipid membrane was detected in an optically trapped Raman microscopy experiment, in which the energy required to deform the vesicle from a spherical shape was related to the energy of trapping the lipid bilayer (48). The forces of optical trapping have also influenced the structure of a thermoresponsive polymer near its critical transition temperature (49). For studies of resonance Raman scattering or surface-enhanced Raman scattering (SERS), particle absorptivity precludes the use of high laser powers for trapping at the Raman excitation wavelength due to heating; for these situations, one may use a long-wavelength, nonresonant laser beam for trapping and another low-power, collinear beam tuned to the electronic or plasmon resonance for probing the Raman scattering (50–53).

2.3. Experimental Arrangements for Optical-Trapping Raman Microscopy

Due to the inefficiency of spontaneous Raman scattering and the limitations on optical power that can be safely focused in a small volume, the detection efficiency of the Raman microscope must be very high. Such high efficiency can be achieved through use of a high-NA, oil-immersion objective (that also achieves tight focusing to increase the gradient force of trapping) coupled to a high–quantum efficiency charge-coupled device (CCD) detector (44, 45). An example of a typical single-beam, optical-trapping Raman microscope is shown in **Figure 3**. The main components are a laser with a high-quality transverse mode, a laser line filter, a beam expander to fill the objective, an epifluorescence microscope frame with a dichroic beam splitter, a high-NA objective, a notch filter, a spectrograph, and a CCD detector.

One notable improvement to the optical train is the addition of a confocal aperture (54, 55) to minimize the collection of light scattered away from the focus of the optical trap (44, 45, 56). The confocal arrangement involves imaging the scattering from the trapped particle through a small aperture matched to the diffraction-limited spot size. The in-focus light passes through the aperture, and much of the out-of-focus scattering originating from above and below the trapped particle is blocked. Confocal light collection is usually achieved through the use of a pinhole, but it may also be achieved (54) by imaging the scattered radiation onto the monochromator entrance slit so as to restrict light collection in the horizontal plane then selectively binning a few rows on the CCD detector to block out-of-focus light in the vertical dimension; see **Figure 3**. Restricting image collection with a confocal aperture provides spatially localized sampling with a volume that can be as small as 1.3 fl (57), and there is minimal interference from the solution surrounding the trapped particle outside this volume. A final addition to a confocal microscope, which is needed for the study of live cells or thermal phase transitions, is temperature control of the

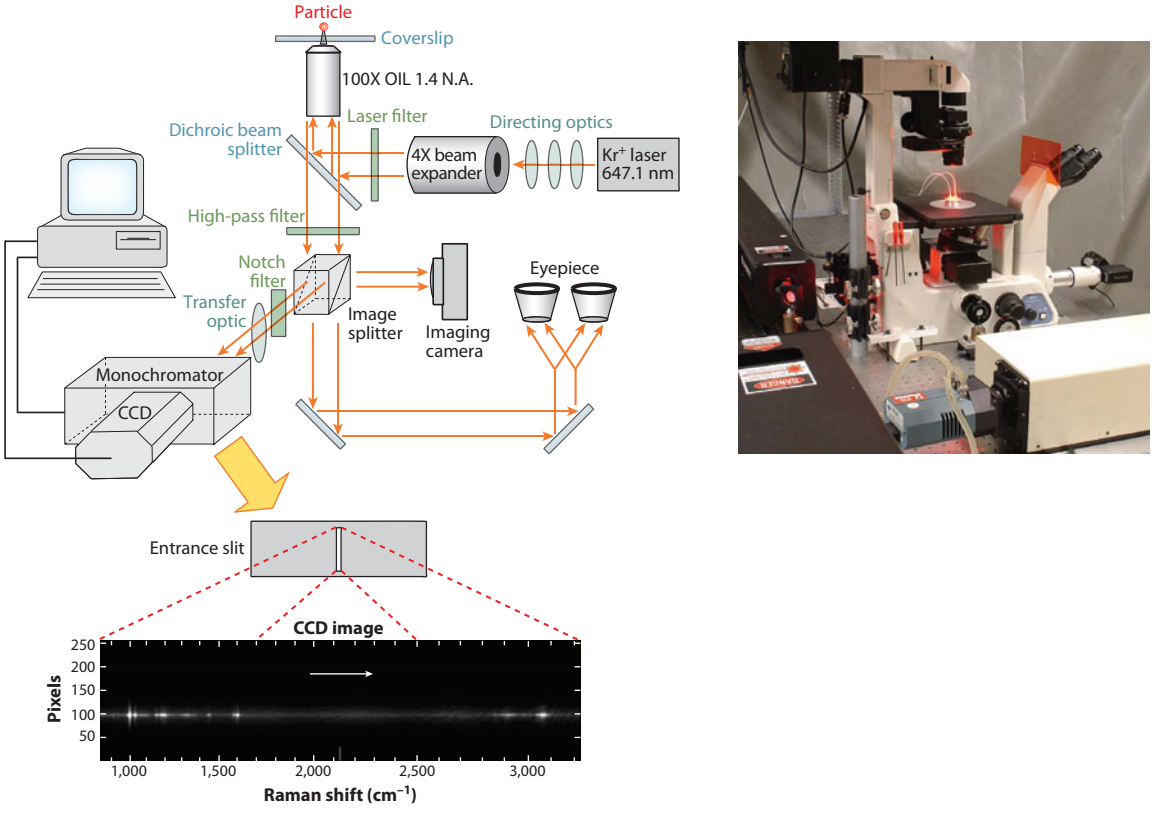

Figure 3

(*Left*) Block diagram and (*right*) photograph of an optical-trapping confocal Raman microscope. The 647.1-nm beam from a krypton-ion laser is brought through the rear port of the microscope, expanded to fill the objective, and brought to a focus in the sample. Scattered radiation is filtered and directed out through a side port, through a notch filter, and into a 0.25-m spectrograph with a charge-coupled device (CCD) detector. (*Inset*) Confocal imaging by the monochromator entrance slit and detector. Block diagram is from Reference 44.

sample. Temperature control can be especially challenging with high-NA oil objectives because the immersion oil is an efficient conductor of heat to the objective, which is in close proximity to the coverslip. A recent study (58) illustrated the problems of temperature control with a typical stage heater, where large, ≥8-K temperature gradients can exist between the heated stage and the solution near the coverslip; these gradients were nearly eliminated with the use of a small-volume, thermally conductive, metal sample cell that was surrounded by a copper block and in contact with a Peltier stage that could either heat or cool the sample (58).

3. APPLICATIONS OF OPTICAL-TRAPPING RAMAN MICROSCOPY

3.1. Raman Microscopy of Emulsion Particles

The first application of optical-trapping Raman microscopy to study particles in liquids was carried out on oil-in-water emulsions by Knoll et al. (59) to obtain information about the molecular structure of microdroplets. Emulsions can be prepared for optical trapping by sonicating mixtures to produce micrometer-sized droplets, which are usually organic droplets suspended in aqueous

solution (60). The organic liquids must have an index of refraction that is greater than that of water so that the particles can be stabilized in an optical trap. It helps if the liquids have a different specific gravity than that of water, which allows the organic droplets to be trapped while the remaining organic and aqueous phases separate, thereby minimizing the interactions with other organic droplets during data acquisition. Because of their spherical shape, optically trapped liquid droplets exhibit morphology-dependent EM resonances, which can be used to determine their size while their composition is monitored with Raman spectroscopy (61). The first use of a near-infrared (Ti:sapphire) laser to prevent fluorescence and photodamage in optical-trapping Raman microscopy was developed and tested on toluene microdroplets; a 1003-cm^{-1} band of a ~10-μm toluene droplet could be measured with a signal-to-noise ratio greater than 250 in a 1-s experiment (56).

Analysis of the contents of a trapped microdroplet in an emulsion is an important application of this tool because differences between a bulk mixture of organic liquids and an emulsion prepared from that mixture can be determined. In one experiment (62), the relative concentrations of *p*-cresol and toluene within emulsion droplets were found to deviate from their bulk concentrations. There was a clear reduction in the amount of *p*-cresol in a picoliter-sized organic droplet in an aqueous solution compared to the bulk *p*-cresol/toluene mixture. Similarly, the feasibility of observing extraction of molecules into single subpicoliter-sized organic droplets has been demonstrated (63). The Raman spectra of a droplet over time showed increasing intensity from *p*-nonylphenol following its addition to the aqueous solution. Data were collected for droplets of various sizes, and the distribution coefficient was greater in microdroplets than in the bulk phases, probably because of preferential adsorption of the solute to the organic/aqueous interface. The results from these experiments are excellent examples of the real-time information that can be obtained from optical-trapping Raman microscopy to determine differences between macroscopic and microscopic sample compositions.

A particularly powerful application of the real-time capabilities of this technique involves monitoring of chemical reactions within an individual, optically trapped emulsion particle. An example is the measurement of polymerization reaction kinetics within a single emulsion particle. During the emulsion polymerization of styrene, the chain reaction was monitored from changes in characteristic C-H stretching modes, and the shrinkage of the particle size by polymerization was determined by measuring morphology-dependent resonances (64, 65). The anionic polymerization of cyanoacrylate monomers conveniently requires water to initiate polymerization. The kinetics of polymerization were determined from decreases in the C = C stretching intensity with time and were compared with polymerization of thin films.

3.2. Raman Microscopy of Dispersed Solid Particles

Applications of optical-trapping Raman microscopy to the study of solid colloidal particles in aqueous dispersion were slow to develop following Thurn & Kiefer's (24) initial demonstration of the technique on glass and quartz particles. More than a decade later, Crawford & Hughes (40, 41) applied optical-trapping Raman microscopy to polystyrene particles and found that the polystyrene degraded upon exposure to only 1.4 mW of 488-nm trapping radiation, which led to broad fluorescence emission from the conjugated degradation products. Although this photochemistry is interesting, these results were not encouraging for experimenters applying optical trapping to probe and not perturb the chemistry of the particle. The application of deep red and near-infrared lasers for trapping solid particles overcame these difficulties for transparent, dielectric particles (44, 45). Ajito & Torimitsu (45) exposed polystyrene latex particles to 120 mW of tightly focused, 730-nm Ti:sapphire laser radiation with no evidence of degradation. The strong

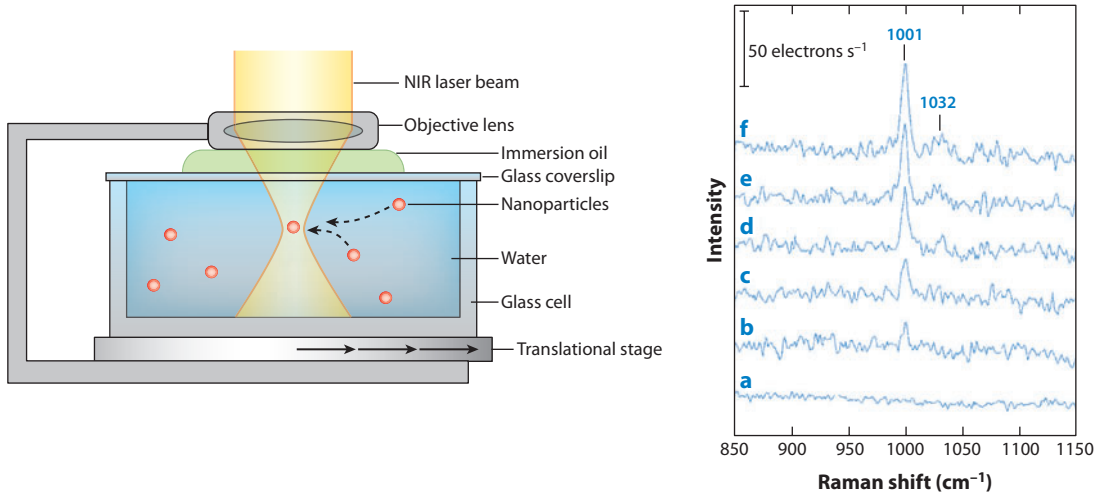

Figure 4

(*Left*) Raman microscopy of 40-nm polystyrene nanoparticles gathered into an optical trap by translating the sample. (*Right*) Increase in Raman scattering intensity as particles accumulate in the optical trap. Spectrum *a* represents the intensity prior to trapping. For spectra *b–f*, the stage is sequentially translated and more particles are being trapped. Abbreviation: NIR, near infrared. Reproduced from Reference 45.

intensity gradient was sufficient to trap 40-nm polystyrene particles, and Raman scattering from a single particle was detected in a 3-s integration. Multiple particles were accumulated into the trap via translation of the sample through laser focus; see **Figure 4**.

Optical trapping can be used to hold and analyze a very small particle from dilute dispersions, allowing one to perform Raman spectroscopy analysis on very small amounts of material. This makes the technique attractive for the pharmaceutical industry as a tool to study new drugs under development. An excellent example of this approach is an investigation (66) of the crystallization kinetics of carbamazepine from methanol under various cooling profiles; the study led to understanding and control over the polymorphic state of the product and required infinitesimal amounts of material. A similar approach was used to characterize the growth of protein crystals needed for X-ray analysis (67). Another critical area of research in the pharmaceutical industry is solid-phase, combinatorial synthesis of drug candidates. The kinetics of reaction steps in a combinatorial synthesis can be monitored in situ on single support particles by optical-trapping Raman microscopy. An example is solid-phase peptide synthesis on amine-primed silica (44), in which time-dependent spectra can be accumulated for both the addition and deprotection steps in peptide synthesis. The deprotection reaction of the N terminus of a bound phenylalanine by cleavage of the FMOC (fluorenylmethyloxycarbonyl) protecting group is shown in **Figure 5**.

Probing gradients in chemical composition within a single particle can be useful for characterizing transport of molecules or understanding how the interior chemistry of a particle differs from its solution interface. Raman microscopy performed with a single-beam optical trap is not well suited to this task because the location of the particle with respect to the laser focus is not easily controlled. This challenge can be solved with a two-laser experiment, which allows independent manipulation of a sample particle relative to the Raman excitation beam (68). An alternative strategy for a single-beam experiment is to allow the particle to settle onto the coverslip or to trap the particle with the laser and bring it into contact with the coverslip. Due to van der Waals interactions (4), particles generally adhere to surfaces, which allows the confocal sampling

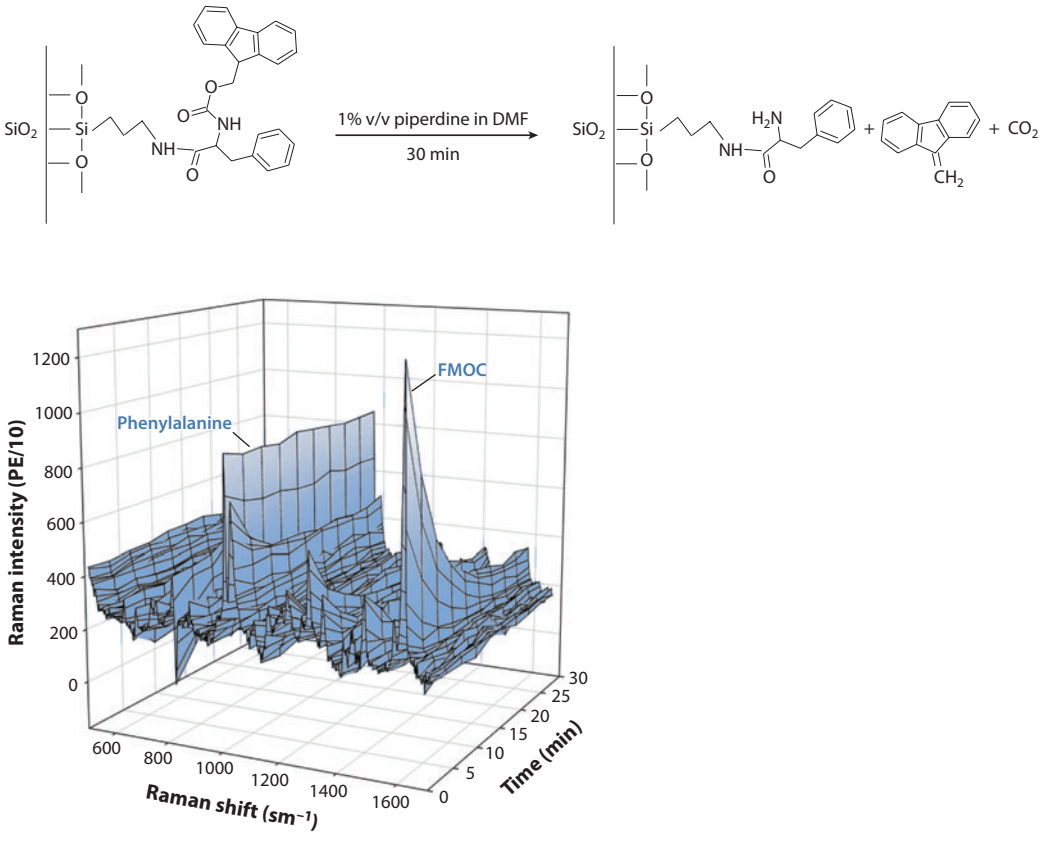

Figure 5

Time-dependent Raman spectra of FMOC being cleaved from phenylalanine bound to a single silica particle. A weighted particle-free solution spectrum is subtracted from all the data. Abbreviations: DMF, dimethylformamide, FMOC, fluorenylmethyloxycarbonyl. Reproduced from Reference 44.

volume to be scanned through an attached particle to profile its composition (57). This approach has been employed to map the transport kinetics of molecules into polymer latex particles (69) and to study the interior solvation environment of C_{18}-functionalized silica particles (70), the wetting-hysteresis behavior of these materials (71), and the membrane and interior composition of phospholipid vesicles (48, 72).

Although the majority of optical-trapping Raman microscopy experiments of solid particles have been performed on transparent or weakly absorbing particles, observing highly scattering or absorbing particles is also of interest. The scattering force on these particles generally overpowers the gradient force of an optical trap so that particles are driven away from the laser source. One approach to examining such particles with a single-beam experiment is to align the trap just below a glass-slide top plate so that the force of scattering is countered by contact with the top plate (73). This arrangement allowed Raman spectra to be acquired for strongly absorbing paint and semiconductor particles and for adsorbates on clusters of silver, allowing the first SERS detection in an optical trap (73); see **Figure 6**. Another approach to SERS detection with optical trapping has been to overcome the strong scattering force from silver particles by partially coating a larger dielectric (SiO_2) sphere with silver, so that the gradient force on the dielectric sphere dominates

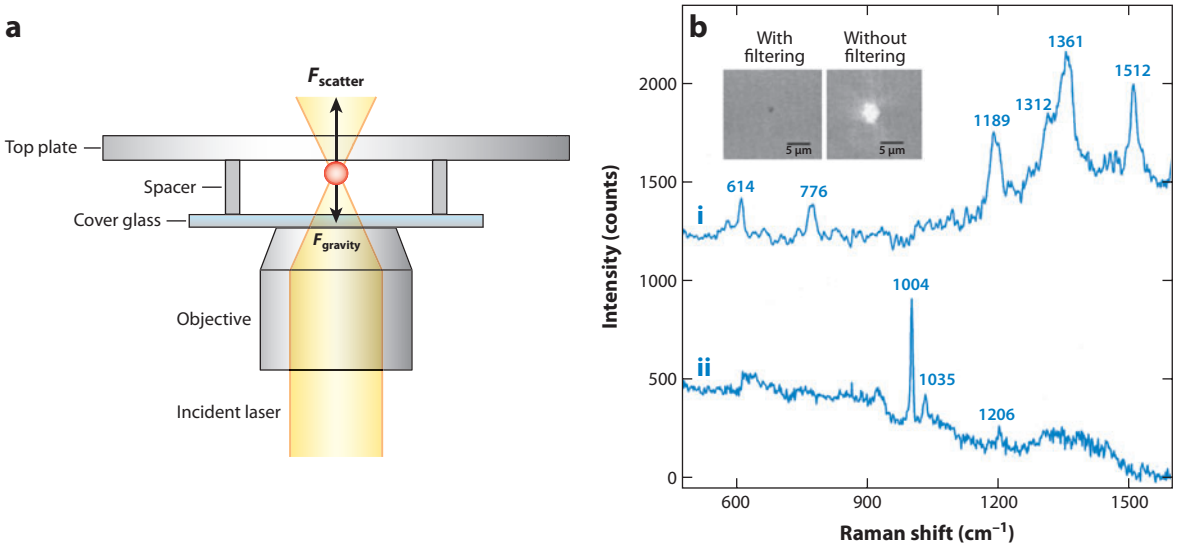

Figure 6

(*a*) Optical trapping of an absorbing particle achieved by forcing the particle against a glass top plate with a spacer and cover glass. (*b*) Surface-enhanced Raman spectra of (*i*) rhodamine 6G and (*ii*) phenylalanine observed from a trapped cluster of silver particles. (*Insets*) A trapped silver cluster recorded (*left*) with filtering and (*right*) without filtering. Reproduced from Reference 73.

(74). This particle structure was also trapped with a 400-mW, nonresonant, 1.06-μm beam and a much lower power (10-μW) 532-nm Raman excitation beam derived from the same laser (75). The arrangement avoids the heating and photodamage (76) that can result from trapping at the plasmon resonance wavelength of silver. Recent results have shown that 1.06-μm radiation can also trap freely dispersed silver nanoparticles, precluding the need for their immobilization on a larger dielectric particle (53); trapping of silver particles by a linearly polarized beam aligns them along the polarization axis and produces a strong SERS signal that can be probed with a 532-nm coaxial laser beam.

3.3. Raman Microscopy of Phospholipid Vesicles

Phospholipid vesicles (also known as liposomes) are stable, spherical structures that are formed in an aqueous solution that contains a lipid-bilayer membrane separating the interior volume from the surrounding solution. Such structures have attracted a great deal of interest as models for biological cells to study the structure and function of biological membranes (77). They are used for encapsulating and delivering small-molecule drugs, oligonucleotides, and therapeutic peptides (78–80) and as mobile-phase additives that modify chromatographic retention of solutes (81–83). Optical-trapping Raman microscopy is a nearly ideal tool for investigating both the molecular contents of lipid vesicles and the structure of the lipid bilayer (84). The energy needed to trap a lipid vesicle originates solely from the phospholipid membrane because the lipid's interior solution is nearly identical to its surroundings. For a 0.6-μm-diameter vesicle, the lipid membrane represents only ~5% of the vesicle volume. Nevertheless, individual, submicrometer-sized vesicles can be trapped indefinitely with modest laser powers (6 mW), producing Raman spectra of the lipid bilayer that provide information about the acyl-chain order and saturation; see **Figure 7**. The permeabilities of vesicle membranes of differing compositions can be compared

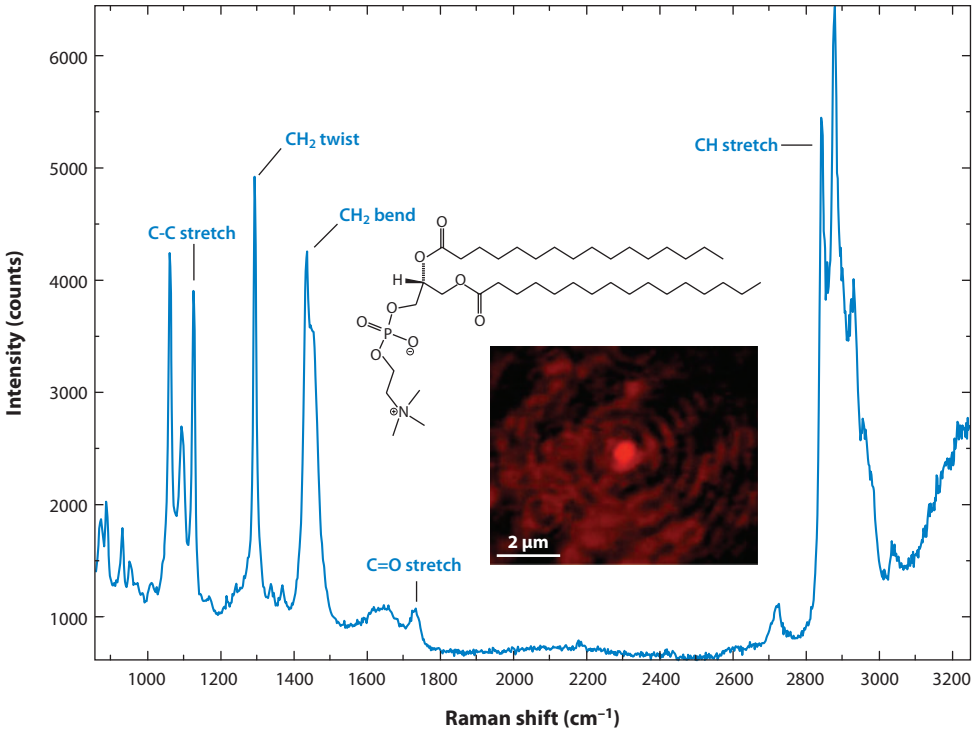

Figure 7

Raman spectrum of a 0.6-μm optically trapped DPPC (1,2-dipalmitoyl-sn-glycero-3-phosphocholine) vesicle excited by a 30-mW laser beam at 647 nm and 3-min integration. The number of DPPC molecules in the vesicle is approximately 10^7. (*Inset*) Image of the trapped vesicle with scattering of the laser beam. Reproduced from Reference 84.

by monitoring the loss of encapsulated neutral molecules or molecular ions as a function of time (84). This methodology can be used to detect cholesterol or small-molecule solutes within the membrane (85) and has been used to determine the membrane permeability, partitioning, and acyl chain–order disruption of nonsteroidal anti-inflammatory (72) and tricyclic antidepressant (86) drugs. Confocal Raman microscopy can elucidate drug-membrane interactions through the use of clinically relevant, low-micromolar concentrations of drugs, and the depletion of drug from solution by membrane partitioning is prevented by working at even lower lipid concentrations.

Raman microscopy of optically trapped vesicles can also be used to study the structure of phospholipid membranes. The force of the optical trap on the vesicle membrane can be sufficient to deform a trapped vesicle from its spherical equilibrium shape and thus can be used to determine the stiffness of a vesicle membrane. Through use of perchlorate ions as a Raman-active marker in the outer solution, the Raman scattering from the phospholipid and outer solution can be monitored over a range of laser powers until a discontinuity in intensity indicates that the vesicle being pinched by the force of the optical trap (48). Structural changes in the phospholipid vesicle membrane as it is passed through temperature-dependent phase transitions can also be measured. A temperature-controlled stage on the confocal-Raman microscope (58) was used to acquire Raman spectra of DPPC (1,2-dipalmitoyl-sn-glycero-3-phosphocholine) vesicles over a range of temperatures from 4°C to 55°C. The spectra were analyzed via self-modeling curve resolution, which revealed subtle

structural changes indicative of sub-, pre-, and main transitions of the membrane (87). Finally, the kinetics of chemical reactions of the lipid membrane, such as the hydrolysis of phospholipids in the bilayer catalyzed by phospholipase A_2 (88), can also be measured by Raman microscopy. Phospholipase enzymes are found in the venom of bees and snakes and are also released in response to inflammation. Raman microscopy can be used to monitor changes in lipid vibrational spectra during hydrolysis and to report reaction kinetics on a single optically trapped vesicle. These kinetics showed an induction period or "lag phase" followed by a rapid "burst phase," during which the reaction velocity corresponded to an enzyme turnover rate of $k_3 = 1.2\ (\pm 0.1) \times 10^3\ s^{-1}$, which agrees with conventional measurements of enzyme activity. In an optical-trapping Raman microscopy experiment, this activity was measured with an average of as few as two enzyme molecules bound to the vesicle under observation.

3.4. Raman Microscopy of Biological Particles

The fastest-growing application of optical-trapping Raman microscopy involves the study of biological particles. Very early in the development of optical trapping, Ashkin and colleagues (17, 89) published pioneering papers establishing the suitability of an optical trap to hold and manipulate living bacteria and yeast cells. These studies revealed the sensitivity of living cells to laser radiation, especially in the visible region, and the much less severe damage caused by trapping with near-infrared radiation. Since that time, optical trapping has been widely used to manipulate biological samples for chemical analysis (21), although until recently it had not been paired with Raman microscopy. The versatility of this Raman microscopy technique has been demonstrated in experiments on living cells, bacteria, spores, intracellular organelles, and protein particles. A review of optical-trapping Raman microscopy of eukaryotic cells addresses issues of maintaining cell viability during these measurements (90). Raman spectroscopy is particularly well suited for analyses of such samples: Structural information is obtained from the vibrational spectrum, while optical trapping immobilizes a sample that might otherwise diffuse (or swim!) from the center of focus.

The first combination of optical trapping and Raman spectroscopy to observe living cells was reported by Xie et al. (91), who investigated both blood and yeast cells. A near-infrared, diode laser beam was used for both optical trapping and Raman excitation to minimize sample heating and maintain cell viability. Spectra from living yeast cells and yeast cells that had been immersed in boiling water were compared, and it was possible to discriminate between them. Heat-induced denaturation of yeast cells and bacteria was studied systematically through introduction of the microorganisms into a temperature-controlled sample cell (92, 93); large changes in the phenylalanine scattering at 1004 cm^{-1} were observed, consistent with changes in protein environment with unfolding. The response of optically trapped yeast cells to hyperosmotic stress conditions has also been studied; in these experiments (94), real-time regulation in the synthesis of ethanol versus glycerol was detected. Changes in the biochemistry of yeast during its cell cycle have also been investigated, and evidence of protein and lipid biosynthesis, along with increases in RNA activity, was found in its lag phase (95).

Optical-trapping Raman microscopy has also been directed toward examining erythrocytes and lymphocytes (i.e., red and white blood cells). Resonance Raman spectra of erythrocytes, which were optically trapped with a near-infrared diode laser and excited with different lines from an argon-ion laser, produced selective resonance enhancement of the heme groups of hemoglobin (51); their vibrations offered information about the oxidation and spin state of the heme irons. The oxygenation cycle of individual, trapped red blood cells was monitored by the same instrument while the solution surrounding the trapped red blood cell was varied (96); different buffers were

transported through the lab-on-a-chip device through the use of electroosmotic flow while the resonance Raman spectrum was collected in real time. Changes in the heme vibrations were indicative of the oxygenation cycle of the cell. A similar dual-laser microscope was used to acquire spectra of red blood cells in their oxygenated, deoxygenated, and carboxy-hemoglobin states (50); cyanide was found to affect the spin-state marker bands of hemoglobin. These experiments showed that different hemoglobin states can be distinguished from one another and that effects of cyanide on oxygen binding can also be detected. The analysis of single lymphocytes by optical-trapping Raman microscopy detected subtle changes in band intensities correlated with T cell blastogenesis (97); differences were also found between rested versus activated thymocytes. Raman microscopy was also used to distinguish normal T and B lymphocytes from healthy subjects with cancer cells from leukemia patients (98); Raman bands associated with DNA and protein vibrations clearly discriminated between the two classes of cells. Principal-components and linear-discriminant analyses successfully classified 90% of cancer patient cells and 95% of normal cells. A follow-up study showed that Raman spectroscopy classification can be adversely impacted by traditional methods of fixing cells (99); optical-trapping Raman microscopy of unfixed cells provided a control for this study and the most accurate discrimination because many vibrational modes that are cancer reporters are changed by the fixation process.

Detection and identification of bacteria and bacterial spores by optical-trapping Raman microscopy have been active areas of investigation. Raman spectra of single bacteria from six different species have been readily classified by principal-components analysis when the cells were synchronized in their growth phases (100); Raman bands associated with amino acids, proteins, lipids, and carbohydrates appear in slightly different ratios in each of the species. Unsynchronized bacteria from random growth phases are more challenging to classify because of variations among individuals of the same species. Protein overexpression by transfected bacteria (typically *Escherichia coli*) is a critical process in the field of biotechnology. Several recent studies (101–103) showed that optical-trapping Raman microscopy can rapidly detect the production of a recombinant protein as it is expressed by a single bacterial cell. Another recent study (104) addressed the lysis of single bacterial cells and found spectral differences between lysis from outside the cell by lysozyme versus from within the cell by a bacteriophage. Driven by security concerns, investigators have recently carried out considerable research to detect and identify bacterial spores by optical-trapping Raman microscopy. Single spores have been trapped and accurately identified directly in solution (105) and through the manipulation of a trapped spore into close proximity to a SERS-active gold-colloid surface to enhance its scattering (106). Calcium dipicolinate, which can represent 5–15% of the dry weight of bacterial spores, is related to the resistance of spores to heat and other environmental stresses; this component was readily quantified in individual spores by a combination of optical-trapping Raman microscopy and microfluidics (107). Calcium dipicolinate is also an important biomarker, released upon germination of bacterial spores, that was measured to study the heterogeneity of germination kinetics of individual spores (108).

A particularly impressive development in optical-trapping Raman microscopy has been the detection and investigation of smaller, subcellular structures. Submicrometer-sized organelles have been successfully trapped and analyzed with Raman spectroscopy (109); specifically, synaptosomes, nerve-ending particles that are approximately 500–700 nm in diameter, isolated from a rat neuron, were trapped with near-infrared radiation and observed without photochemical degradation. In a follow-up study (110), the release of glutamate by a single synaptosome in response to the addition of a K^+-channel blocker was monitored over time, and the measured changes in Raman scattering corresponded to the release of ~3 amol of glutamate; see **Figure 8**. Individual mitochondria have been isolated from rat tissue and trapped; their Raman spectra were observed following the addition of calcium ion to the surrounding solution (111). Optical-trapping Raman microscopy can be also

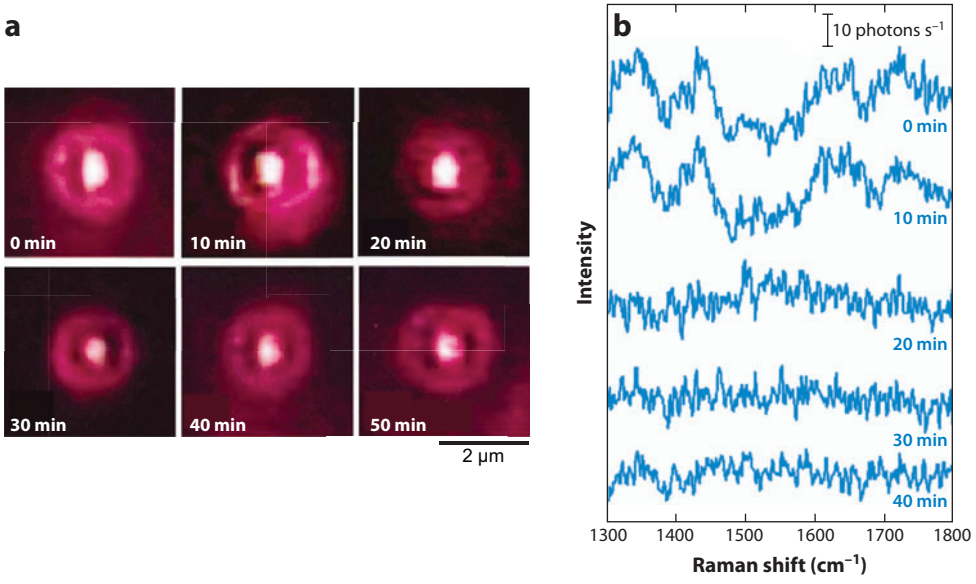

Figure 8

(*a*) Images of a trapped synaptosome. (*b*) Time-dependent Raman spectra of a single synaptosome following the addition of 10 μM 4-aminopyridine. Reproduced from Reference 110.

used to analyze individual protein aggregates; for example, individual very low density lipoprotein aggregates were isolated from human serum samples, and information about their composition was obtained. Specifically, free saturated fatty acids formed highly ordered domains in samples from subjects whose diet was higher in saturated fat (112); the hydrolysis of lipoprotein particles was monitored in vitro following the addition of lipoprotein lipase, demonstrating the feasibility of measuring the kinetics of lipid metabolism. Aggregates of α-elastin have also been trapped and investigated; the size of the trapped protein aggregate was determined from its thermal motion in the trap (113). Finally, optical-trapping Raman microscopy has been employed to identify, without staining, human chromosomes extracted from peripheral blood samples (114); following Raman spectroscopy analysis, the trapped chromosome was maneuvered and fixed to the coverslip surface, where conventional cytogenetic analysis validated its identity.

This last experiment (114) illustrates the unique capabilities provided by a combination of Raman microscopy analysis and sample manipulation with the optical trap. First, an optical trap can be used to accumulate cells from a low-concentration sample, thereby increasing the sensitivity of the measurement. This was first demonstrated on polystyrene nanoparticles (45) and more recently on red blood and yeast cells (115). In a study of the ability to use Raman spectra to discriminate between live versus dead yeast cells (116), manipulation of the cells with the optical trap into a collection chamber allowed the classification to be validated by standard staining methods. A two-beam optical trap was formed from a 1.06-μm ytterbium laser and combined with a 785-nm, diode laser beam for Raman excitation to acquire spectra of local regions within large (30-μm) human keratinocytes (117). This device and a single-beam optical-trapping microscope have been combined with microfluidic sample handling to sort leukemia cells (117, 118). Bacterial and yeast cells have been sorted by uptake of ^{13}C glucose through its conversion to ^{13}C phenylalanine, which was detected by its Raman scattering intensity; the sorted cells were then recovered by incubation and tested for their genetic makeup (119).

4. SUMMARY AND FUTURE PROSPECTS

The combination of optical-trapping and confocal Raman microscopy has introduced a vibrational spectroscopy tool into the field of colloidal particle analysis. This method can provide in situ molecular structure information on the composition and reactivity of individual suspended particles, and it has been applied to emulsion chemistry, materials analysis, solid-phase synthesis, liposomes, biotechnology, and clinical assays. Single particles can be trapped and analyzed from small-volume (submicroliter) samples of very dilute (10^6 particles ml^{-1}) dispersions. Because a trapped particle can be manipulated in a small-volume environment, vibrational spectroscopy analysis can be combined with sorting for further analysis or testing. Optical-trapping Raman microscopy follows the tradition of microchemical analysis (120), which began with the adaptation of wet chemical methods to optical microscopy for the analysis of nanogram-to-picogram-sized samples; the Raman spectrum is replacing colorimetric or gravimetric reagents. Despite the achievements of this methodology, there are limitations to single-particle measurements. Specifically, these measurements are serial determinations in which information is gathered one particle at a time. A recent paper (121) considered this limitation with respect to single-cell experiments, raising the question of whether a representative cell can be sampled for analysis. The probability of a successful outcome of such an analysis depends on the inhomogeneity in particle or cell populations, which can only be assessed with multiple measurements to characterize distributions, followed by application of statistical criteria to set a minimum number of particles needed to obtain meaningful results. To address this challenge, significantly greater effort will be required to develop automated sample-handling, -trapping, and -analysis methods and to enable the routine characterization of particle-composition distributions.

DISCLOSURE STATEMENT

The authors are not aware of any affiliations, memberships, funding, or financial holdings that might be perceived as affecting the objectivity of this review.

ACKNOWLEDGMENTS

This research was supported in part with funds from the National Science Foundation under grants CHE-0137569 and CHE-0654229 and from the U.S. Department of Energy under grant DE-FG03-93ER14333. D.P.C.'s current affiliation is: Advanced Characterization Department, ExxonMobil Chemical Company, Baytown, Texas 77520.

LITERATURE CITED

1. Cosgrove T. 2005. *Colloid Science: Principles, Methods, and Applications*. Oxford: Blackwell
2. Panyam J, Labhasetwar V. 2003. Biodegradable nanoparticles for drug and gene delivery to cells and tissue. *Adv. Drug Deliv. Rev.* 55:329–47
3. Boldi AM, ed. 2006. *Combinatorial Synthesis of Natural Product–Based Libraries*. Boca Raton: CRC
4. Ross S, Morrison ID. 1988. *Colloidal Systems and Interfaces*. New York: Wiley
5. Stumm W. 1992. *Chemistry of the Solid-Water Interface: Processes at the Mineral-Water and Particle-Water Interface in Natural Systems*. New York: Wiley
6. Brinker CJ. 1996. Porous inorganic materials. *Curr. Opin. Solid State Mater. Sci.* 1:798–805
7. Giddings JC. 1992. *Unified Separation Science*. New York: Wiley Intersci.
8. Pecora R. 1985. *Dynamic Light Scattering: Applications of Photon Correlation Spectroscopy*. New York: Plenum
9. Schärtl W. 2007. *Light Scattering from Polymer Solutions and Nanoparticle Dispersions*. Berlin: Springer

10. Raman CV, Krishnan KS. 1928. A new type of secondary radiation. *Nature* 121:501–2
11. Pelletier MJ, ed. 1991. *Analytical Raman Spectroscopy*. Oxford: Blackwell
12. Puppels GJ, Colier W, Olminkhof JHF, Otto C, de Mul FFM, Greve J. 1991. Description and performance of a highly sensitive confocal Raman microspectrometer. *J. Raman Spectrosc.* 22:217–25
13. Ashkin A. 1970. Acceleration and trapping of particles by radiation pressure. *Phys. Rev. Lett.* 24:156
14. Ashkin A, Dziedzic JM, Bjorkholm JE, Chu S. 1986. Observation of a single-beam gradient force optical trap for dielectric particles. *Opt. Lett.* 11:288
15. Ashkin A. 1992. Forces of a single-beam gradient laser trap on a dielectric sphere in the ray optics regime. *Biophys. J.* 61:569–82
16. Ashkin A. 2000. History of optical trapping and manipulation of small-neutral particle, atoms, and molecules. *IEEE J. Sel. Top. Quantum Electron.* 6:841–56
17. Ashkin A, Dziedzic JM. 1987. Optical trapping and manipulation of viruses and bacteria. *Science* 235:1517–20
18. Chiu DT, Hsiao A, Gaggar A, Garza-Lopez RA, Orwar O, Zare RN. 1997. Injection of ultrasmall samples and single molecules into tapered capillaries. *Anal. Chem.* 69:1801–7
19. Grover SC, Skirtach AG, Gauthier RC, Grover CP. 2001. Automated single-cell sorting system based on optical trapping. *J. Biomed. Opt.* 6:14–22
20. Stout AL. 2001. Detection and characterization of individual intermolecular bonds using optical tweezers. *Biophys. J.* 80:2976–86
21. Kuyper CL, Chiu DT. 2002. Optical trapping: a versatile technique for biomanipulation. *Appl. Spectrosc.* 56:300–12A
22. Kitamura N, Kitagawa F. 2003. Optical trapping—chemical analysis of single microparticles in solution. *J. Photochem. Photobiol. C Photochem. Rev.* 4:227–47
23. Moffitt JR, Chemla YR, Smith SB, Bustamante C. 2008. *Annu. Rev. Biochem.* 77:205–28
24. Thurn R, Kiefer W. 1984. Raman-microsampling technique applying optical levitation by radiation pressure. *Appl. Spectrosc.* 38:78–83
25. Thurn R, Kiefer W. 1985. Structural resonances observed in the Raman spectra of optically levitated liquid droplets. *Appl. Opt.* 24:1515–19
26. Preston RE, Lettieri TR, Semerjian HG. 1985. Characterization of single levitated droplets by Raman spectroscopy. *Langmuir* 1:365–67
27. Hopkins RJ, Mitchem L, Ward AD, Reid JP. 2004. Control and characterization of a single aerosol droplet in a single-beam gradient-force optical trap. *Phys. Chem. Chem. Phys.* 6:4924–27
28. Kaiser T, Roll G, Schweiger G. 1996. Investigation of coated droplets in an optical trap: Raman-scattering, elastic-light-scattering, and evaporation characteristics. *Appl. Opt.* 35:5918–24
29. Esen C, Kaiser T, Schweiger G. 1996. Raman investigation of photopolymerization reactions of single optically levitated microparticles. *Appl. Spectrosc.* 50:823–28
30. Music J, Popp J, Trunk M, Kiefer W. 1998. Investigations of radical polymerization and copolymerization reactions in optically levitated microdroplets by simultaneous Raman spectroscopy, Mie scattering, and radiation pressure measurements. *Appl. Spectrosc.* 52:692–701
31. Rassat SD, Davis EJ. 1994. Temperature measurement of single levitated microparticles using Stokes/anti-Stokes Raman intensity ratios. *Appl. Spectrosc.* 48:1498–505
32. Lübben JF, Mund C, Schrader B, Zellner R. 1999. Uncertainties in temperature measurements of optically levitated single aerosol particles by Raman spectroscopy. *J. Mol. Struct.* 480/481:311–16
33. Kaiser T, Roll G, Schweiger G. 1995. Enhancement of the Raman spectrum of optically levitated microspheres by seeded nanoparticles. *J. Opt. Soc. Am. B* 12:281–86
34. Kiefer W, Popp J, Lankers M, Trunk M, Hartmann I, et al. 1997. Raman-Mie scattering from single laser trapped microdroplets. *J. Mol. Struct.* 408/409:113–20
35. Reid JP, Mitchem L. 2006. Laser probing of single-aerosol droplet dynamics. *Annu. Rev. Phys. Chem.* 57:245–71
36. Wright WH, Sonek GJ, Berns MW. 1993. Radiation trapping forces on microspheres with optical tweezers. *Appl. Phys. Lett.* 63:715–17
37. Malagnino N, Pesce G, Sasso A, Arimondo E. 2002. Measurements of trapping efficiency and stiffness in optical tweezers. *Opt. Commun.* 214:15–24

38. Bartlett P, Henderson S. 2002. Three-dimensional force calibration of a single-beam optical gradient trap. *J. Phys. Condens. Matter* 14:7757–68
39. Barton JP, Alexander DR, Schaub SA. 1988. Internal and near-surface electromagnetic fields for a spherical particle irradiated by a focused laser beam. *J. Appl. Phys.* 64:1632–39
40. Crawford KD, Hughes KD. 1997. Rapid formation and spectroscopic observation of polystyrene conjugation in individual micron-diameter particles with visible radiation. *J. Phys. Chem. B* 101:864–70
41. Crawford KD, Hughes KD. 1998. Raman vibrational evidence for the presence of conjugated regions in individual micron diameter polystyrene particles irradiated with visible radiation. *J. Phys. Chem. B* 102:2325–28
42. Celliers PM, Conia J. 2000. Measurement of localized heating in the focus of an optical trap. *Appl. Opt.* 39:3396–407
43. Curcio JA, Petty CC. 1951. The near infrared absorption spectrum of liquid water. *J. Opt. Soc. Am.* 41:302
44. Houlne MP, Sjostrom CM, Uibel RH, Kleimeyer JA, Harris JM. 2002. Confocal Raman microscopy for monitoring chemical reactions on single optically trapped, solid-phase support particles. *Anal. Chem.* 74:4311–19
45. Ajito K, Torimitsu K. 2002. Single nanoparticle trapping using a Raman tweezers microscope. *Appl. Spectrosc.* 56:541–44
46. Bar-Ziv R, Menes R, Moses E, Safran SA. 1995. Local unbinding of pinched membranes. *Phys. Rev. Lett.* 75:3356
47. Bar-Ziv R, Moses E, Nelson P. 1998. Dynamic excitations in membranes induced by optical tweezers. *Biophys. J.* 75:294–320
48. Cherney DP, Bridges TE, Harris JM. 2004. Optical trapping of unilamellar phospholipid vesicles: investigation of the effect of optical forces on the lipid membrane shape by confocal-Raman microscopy. *Anal. Chem.* 76:4920–28
49. Tsuboi Y, Nishino M, Sasaki T, Kitamura N. 2005. Poly(*N*-isopropylacrylamide) microparticles produced by radiation pressure of a focused laser beam: a structural analysis by confocal Raman microspectroscopy combined with a laser-trapping technique. *J. Phys. Chem. B* 109:7033–39
50. Geßner R, Winter C, Rösch P, Schmitt M, Petry R, et al. 2004. Identification of biotic and abiotic particles by using a combination of optical tweezers and in situ Raman spectroscopy. *ChemPhysChem* 5:1159–70
51. Ramser K, Logg K, Goksor M, Enger J, Kall M, Hanstorp D. 2004. Resonance Raman spectroscopy of optically trapped functional erythrocytes. *J. Biomed. Opt.* 9:593–600
52. Svedberg F, Käll M. 2006. On the importance of optical forces in surface-enhanced Raman scattering (SERS). *Faraday Discuss.* 132:35–44
53. Tanaka Y, Yoshikawa H, Itoh T, Ishikawa M. 2009. Surface enhanced Raman scattering from pseudoisocyanine on Ag nanoaggregates produced by optical trapping with a linearly polarized laser beam. *J. Phys. Chem. C* 113:11856–60
54. Williams KPJ, Pitt GD, Batchelder DN, Kip BJ. 1994. Confocal Raman microspectroscopy using a stigmatic spectrograph and CCD detector. *Appl. Spectrosc.* 48:232–35
55. Schrum KF, Ko SH, Ben-Amotz D. 1996. Description and theory of a fiber-optic confocal and superfocal Raman microspectrometer. *Appl. Spectrosc.* 50:1150–55
56. Ajito K. 1998. Combined near-infrared Raman microprobe and laser trapping system: application to the analysis of a single organic microdroplet in water. *Appl. Spectrosc.* 52:339–42
57. Bridges TE, Houlne MP, Harris JM. 2003. Spatially resolved analysis of small particles by confocal Raman microscopy: depth profiling and optical trapping. *Anal. Chem.* 76:576–84
58. Fox CB, Myers GA, Harris JM. 2007. Temperature-controlled confocal Raman microscopy to detect phase transitions in phospholipid vesicles. *Appl. Spectrosc.* 61:465–69
59. Knoll P, Marchl M, Kiefer W. 1988. Raman spectroscopy of microparticles in laser light traps. *Ind. J. Pure Appl. Phys.* 26:268–77
60. Lankers M, Popp J, Urlaub E, Stahl H, Rößling G, Kiefer W. 1995. Investigations of multiple component systems by means of optical trapping and Raman spectroscopy. *J. Mol. Struct.* 348:265–68

61. Lankers M, Popp J, Kiefer W. 1994. Raman and fluorescence spectra of single optically trapped microdroplets in emulsions. *Appl. Spectrosc.* 48:1166–68
62. Ajito K, Morita M. 1999. Imaging and spectroscopic analysis of single microdroplets containing *p*-cresol using the near-infrared laser tweezers/Raman microprobe system. *Surf. Sci.* 427–428:141–46
63. Ajito K, Morita M, Torimitsu K. 2000. Investigation of the molecular extraction process in single subpicoliter droplets using a near-infrared laser Raman trapping system. *Anal. Chem.* 72:4721–25
64. Urlaub E, Lankers M, Hartmann I, Popp J, Trunk M, Kiefer W. 1994. Raman investigation of styrene polymerization in single optically trapped emulsion particles. *Chem. Phys. Lett.* 231:511–14
65. Urlaub E, Lankers M, Hartmann I, Popp J, Trunk M, Kiefer W. 1996. Applications of the optical trapping technique to analyze chemical reactions in single emulsion particles. *Fresenius J. Anal. Chem.* 355:329–31
66. Anquetil PA, Brenan CJH, Marcolli C, Hunter IW. 2003. Laser Raman spectroscopic analysis of polymorphic forms in microliter fluid volumes. *J. Pharm. Sci.* 92:149–60
67. Noda K, Sato H, Watanabe S, Yokoyama S, Tashiro H. 2007. Efficient characterization for protein crystals using confocal Raman spectroscopy. *Appl. Spectrosc.* 61:11–18
68. Rusciano G, De Luca AC, Sasso A, Pesce G. 2006. Phase-sensitive detection in Raman tweezers. *Appl. Phys. Lett.* 89:261116
69. Bridges TE, Uibel RH, Harris JM. 2006. Measuring diffusion of molecules into individual polymer particles by confocal Raman microscopy. *Anal. Chem.* 78:2121–29
70. Gasser-Ramirez JL, Harris JM. 2009. Confocal Raman microscopy of the interfacial regions of liquid chromatographic stationary-phase materials. *Anal. Chem.* 81:2869–76
71. Gasser-Ramirez JL, Harris JM. 2009. Confocal Raman microscopy investigation of the wetting of reversed-phase liquid chromatographic stationary phase particles. *Anal. Chem.* 81:7632–38
72. Fox CB, Horton RA, Harris JM. 2006. Detection of drug-membrane interactions in individual phospholipid vesicles by confocal Raman microscopy. *Anal. Chem.* 78:4918–24
73. Xie C, Li Y-Q. 2002. Raman spectra and optical trapping of highly refractive and nontransparent particles. *Appl. Phys. Lett.* 81:951–53
74. Jordan P, Cooper J, McNay G, Docherty FT, Smith WE, et al. 2004. Three-dimensional optical trapping of partially silvered silica microparticles. *Opt. Lett.* 29:2488–90
75. Jordan P, Cooper J, McNay G, Docherty F, Graham D, et al. 2005. Surface-enhanced resonance Raman scattering in optical tweezers using coaxial second harmonic generation. *Opt. Express* 13:4148–53
76. King MD, Khadka S, Craig GA, Mason MD. 2008. Effect of local heating on the SERS efficiency of optically trapped prismatic nanoparticles. *J. Phys. Chem. C* 112:11751–57
77. Torchilin V, Weissig V. 2003. *Liposomes: A Practical Approach*. Oxford: Oxford Univ. Press
78. Wang G. 2005. Liposome as drug delivery vehicles. In *Drug Delivery: Principles and Applications*, ed. B Wang, TJ Siahaan, RA Soltero, pp. 411–34. Hoboken: Wiley
79. Soni V, Kohli DV, Jain SK. 2005. Transferrin coupled liposomes as drug delivery carrier for brain targeting of 5-florouracil. *J. Drug Target.* 13:245–50
80. Samad A, Sultana Y, Aqil M. 2007. Liposomal drug delivery systems: an update review. *Curr. Drug Deliv.* 4:297–305
81. Carrozzino JM, Khaledi MG. 2005. pH effects on drug interactions with lipid bilayers by liposome electrokinetic chromatography. *J. Chromatogr. A* 1079:307–16
82. Bilek G, Kremser L, Blaas D, Kenndler E. 2006. Analysis of liposomes by capillary electrophoresis and their use as carrier in electrokinetic chromatography. *J. Chromatogr. B* 841:38–51
83. Wang Y, Sun J, Liu H, Wang Y, He Z. 2007. Prediction of human drug absorption using liposome electrokinetic chromatography. *Chromatographia* 65:173–77
84. Cherney DP, Conboy JC, Harris JM. 2003. Optical-trapping Raman microscopy detection of single unilamellar lipid vesicles. *Anal. Chem.* 75:6621–28
85. Sanderson JM, Ward AD. 2004. Analysis of liposomal membrane composition using Raman tweezers. *Chem. Commun.* 2004:1120–21
86. Fox CB, Harris JM. 2009. Confocal Raman microscopy for simultaneous monitoring of partitioning and disordering of tricyclic antidepressants in phospholipid vesicle membranes. *J. Raman Spectrosc.* 41:498–507

87. Fox CB, Uibel RH, Harris JM. 2007. Detecting phase transitions in phosphatidylcholine vesicles by Raman microscopy and self-modeling curve resolution. *J. Phys. Chem. B* 111:11428–36
88. Cherney DP, Myers GA, Horton RA, Harris JM. 2006. Optically trapping confocal Raman microscopy of individual lipid vesicles: kinetics of phospholipase A2–catalyzed hydrolysis of phospholipids in the membrane bilayer. *Anal. Chem.* 78:6928–35
89. Ashkin A, Dziedzic JM, Yamane T. 1987. Optical trapping and manipulation of single cells using infrared laser beams. *Nature* 330:769–71
90. Snook RD, Harvey TJ, Faria EC, Gardner P. 2009. Raman tweezers and their application to the study of singly trapped eukaryotic cells. *Integr. Biol.* 1:43–52
91. Xie C, Dinno MA, Li Y-Q. 2002. Near-infrared Raman spectroscopy of single optically trapped biological cells. *Opt. Lett.* 27:249–51
92. Xie C, Li Y-Q, Tang W, Newton RJ. 2003. Study of dynamical process of heat denaturation in optically trapped single microorganisms by near-infrared Raman spectroscopy. *J. Appl. Phys.* 94:6138–42
93. Xie C, Goodman C, Dinno M, Li Y-Q. 2004. Real-time Raman spectroscopy of optically trapped living cells and organelles. *Opt. Express* 12:6208–14
94. Singh GP, Creely CM, Volpe G, Grotsch H, Petrov D. 2005. Real-time detection of hyperosmotic stress response in optically trapped single yeast cells using Raman microspectroscopy. *Anal. Chem.* 77:2564–68
95. Singh GP, Volpe G, Creely CM, Grötsch H, Geli IM, Petrov D. 2006. The lag phase and G1 phase of a single yeast cell monitored by Raman microspectroscopy. *J. Raman Spectrosc.* 37:858–64
96. Ramser K, Enger J, Goksör M, Hanstorp D, Logg K, Käll M. 2005. A microfluidic system enabling Raman measurements of the oxygenation cycle in single optically trapped red blood cells. *Lab Chip* 5:431–36
97. Mannie MD, McConnell TJ, Xie C, Li Y-Q. 2005. Activation-dependent phases of T cells distinguished by use of optical tweezers and near infrared Raman spectroscopy. *J. Immunol. Methods* 297:53–60
98. Chan JW, Taylor DS, Lane SM, Zwerdling T, Tuscano J, Huser T. 2008. Nondestructive identification of individual leukemia cells by laser trapping Raman spectroscopy. *Anal. Chem.* 80:2180–87
99. Chan JW, Taylor DS, Thompson DL. 2009. The effect of cell fixation on the discrimination of normal and leukemia cells with laser tweezers Raman spectroscopy. *Biopolymers* 91:132–39
100. Xie C, Mace J, Dinno MA, Li YQ, Tang W, et al. 2005. Identification of single bacterial cells in aqueous solution using confocal laser tweezers Raman spectroscopy. *Anal. Chem.* 77:4390–97
101. Ramser K, Wenseleers W, Dewilde S, Van Doorslaer S, Moens L, Hanstorp D. 2007. Micro-resonance Raman study of optically trapped *Escherichia coli* cells overexpressing human neuroglobin. *J. Biomed. Opt.* 12:044009
102. Xie C, Nguyen N, Zhu Y, Li Y-Q. 2007. Detection of the recombinant proteins in single transgenic microbial cell using laser tweezers and Raman spectroscopy. *Anal. Chem.* 79:9269–75
103. Chan JW, Winhold H, Corzett MH, Ulloa JM, Cosman M, et al. 2007. Monitoring dynamic protein expression in living *E. coli* bacterial cells by laser tweezers Raman spectroscopy. *Cytometry* 71A:468–74
104. Chen D, Shelenkova L, Li Y, Kempf CR, Sabelnikov A. 2009. Laser tweezers Raman spectroscopy potential for studies of complex dynamic cellular processes: single cell bacterial lysis. *Anal. Chem.* 81:3227–38
105. Chan JW, Esposito AP, Talley CE, Hollars CW, Lane SM, Huser T. 2004. Reagentless identification of single bacterial spores in aqueous solution by confocal laser tweezers Raman spectroscopy. *Anal. Chem.* 76:599–603
106. Alexander TA, Pellegrino PM, Gillespie JB. 2003. Near-infrared surface-enhanced Raman scattering–mediated detection of single optically trapped bacterial spores. *Appl. Spectrosc.* 57:1340–45
107. Huang S-S, Chen D, Pelczar PL, Vepachedu VR, Setlow P, Li Y-Q. 2007. Levels of Ca^{2+}-dipicolinic acid in individual *Bacillus* spores determined using microfluidic Raman tweezers. *J. Bacteriol.* 189:4681–87
108. Chen D, Huang S-S, Li Y-Q. 2006. Real-time detection of kinetic germination and heterogeneity of single *Bacillus* spores by laser tweezers Raman spectroscopy. *Anal. Chem.* 78:6936–41
109. Ajito K, Torimitsu K. 2002. Laser trapping and Raman spectroscopy of single cellular organelles in the nanometer range. *Lab Chip* 2:11–14
110. Ajito K, Han C, Torimitsu K. 2004. Detection of glutamate in optically trapped single nerve terminals by Raman spectroscopy. *Anal. Chem.* 76:2506–10

111. Tang H, Yao H, Wang G, Wang Y, Li Y-Q, Feng M. 2007. NIR Raman spectroscopic investigation of single mitochondria trapped by optical tweezers. *Opt. Express* 15:12708–16
112. Chan JW, Motton D, Rutledge JC, Keim NL, Huser T. 2005. Raman spectroscopic analysis of biochemical changes in individual triglyceride-rich lipoproteins in the pre- and postprandial state. *Anal. Chem.* 77:5870–76
113. Mao H, Luchette P. 2008. An integrated laser-tweezers instrument for microanalysis of individual protein aggregates. *Sens. Actuators B Chem.* 129:764–71
114. Ojeda JF, Xie C, Li Y-Q, Bertrand FE, Wiley J, McConnell TJ. 2006. Chromosomal analysis and identification based on optical tweezers and Raman spectroscopy. *Opt. Express* 14:5385–93
115. Jess PRT, Garcés-Chávez V, Riches AC, Herrington CS, Dholakia K. 2007. Simultaneous Raman microspectroscopy of optically trapped and stacked cells. *J. Raman Spectrosc.* 38:1082–88
116. Xie C, Chen D, Li Y-Q. 2005. Raman sorting and identification of single living micro-organisms with optical tweezers. *Opt. Lett.* 30:1800–2
117. Jess PRT, Garcés-Chávez V, Smith D, Mazilu M, Paterson L, et al. 2006. Dual beam fiber trap for Raman microspectroscopy of single cells. *Opt. Express* 14:5779–91
118. Lau AY, Lee LP, Chan JW. 2008. An integrated optofluidic platform for Raman-activated cell sorting. *Lab Chip* 8:1116–20
119. Huang WE, Ward AD, Whiteley AS. 2009. Raman tweezers sorting of single microbial cells. *Environ. Microbiol. Rep.* 1:44–49
120. Benedetti-Pichler AA. 1958. Chemical experimentation under the microscope. *Microchem. J.* 2:3–20
121. Sabelnikov A, Kempf CR. 2008. Single-cell research: What determines its feasibility? *Anal. Biochem.* 383:346–48

Annual Review of
Analytical Chemistry

Volume 3, 2010

Contents

Indexes

Errata

An online log of corrections to *Annual Review of Analytical Chemistry* articles may be found at http://arjournals.annualreviews.org/errata/anchem.